Turbidity currents and submarine morphodynamics

River, Coastal and Estuarine Morphodynamics: RCEM 2005 – Parker & García (eds)

Incision dynamics and shear stress measurements in submarine channels experiments

P. Lancien, F. Métivier & E. Lajeunesse
Institut de Physique du Globe de Paris, France

M.C. Cacas
Institut Français du Pétrole, France

ABSTRACT: We report observations on the incision dynamics of subaqueous channels in small-scale laboratory experiments, showing the initial incision phase, followed by a widening phase associated with an erosion-deposition wave progradation. In order to better characterize the inception phase, we make measurements on the gravity current prior to incision. Thanks to the particle-with-shadow tracking, a new technique using settling particles to gather information on the velocity field, we obtain the lowest part of the downstream velocity vertical profile with a good accuracy. The velocity gradient in the viscous sublayer gave us access to the first direct shear stress measurements in a gravity current.

1 INTRODUCTION

Submarine channels systems are the conduits that allow turbidity currents to transport and deposit material eroded from the continents in the deep sea. However, little is known about the physical processes of their formation, and consequential questions remain unsolved: what are the physical conditions and the dynamics of submarine erosional channels inception? Are they produced by catastrophic flood events or could a steady-state sediment-charged current be sufficient? What are the velocities and densities required to erode? In other terms, what is the necessary shear stress distribution on the bed? How does the channel select his width and his depth?

The lack of answers is mainly due to the difficulty in making measurements on active or abandoned channels, and the probably long time scale needed to develop these structures compared to a human time scale. Because of these drawbacks, researchers have focused on experimental and numerical studies of turbidity currents (Kneller et al. 1999, Kneller & Buckee 2000).

Métivier et al. (2005) managed to reproduce subaqueous channels in small-scale laboratory experiments. This paper complements this previous work, focusing on the description of some incision dynamics aspects and introducing velocity profiles and shear stress measurements.

2 EXPERIMENTAL SETUP

The experimental setup consists of a 100×50 cm incline, immersed in a $200 \times 50 \times 50$ cm flume filled with fresh water mixed with fine particles. Once the powder has settled, a layer is slowly raked upward on the incline to drape it by a uniform sediment blanket. Then, a sustained gravity current is injected at the top of the ramp and flows over this erodible bed. We control the three main parameters of the experiment: the slope of the plane, the input flow rate, and the input flow specific gravity.

The visualization is made from above, using two different devices depending on the time scale of the event type we want to study. For the capture of long time scale events, like the channel formation, a digital camera is used to take one picture each minute. For short time scale events, like the particles transport, close movies of the plane are taken, using a video camera instead.

This setup is rather simple, but the experimental difficulties lie in the choices made for the nature of the sediments and the density current.

2.1 *The sediments*

The particles composing the sediment blanket are made of a mixture of plastic polymer and titanium oxide, achieving a density of $1080\,\mathrm{kg/m^3}$. Most of the grain diameters are comprised between 15 and 40

Figure 1. Typical channel and frontal lobe obtained with our experimental setup. The current inlet is visible at the top.

microns. Their low specific gravity in the water, combined with their small size, make these particles very easily erodible.

2.2 *The gravity current*

The turbidity current is simulated using salt water, without particles. Indeed it is the density contrast which is responsible for the erosional power of the turbidites. In nature, sediments play an indirect role for the erosion, in the sense that they induce this density contrast.

Using the settling velocity V_s, the typical velocity of the density current U, and its typical height H, it is possible to construct a characteristic length:

$$X = \frac{UH}{V_s}$$

X is a settling length; it's the typical horizontal distance a suspended particle of the density current can achieve

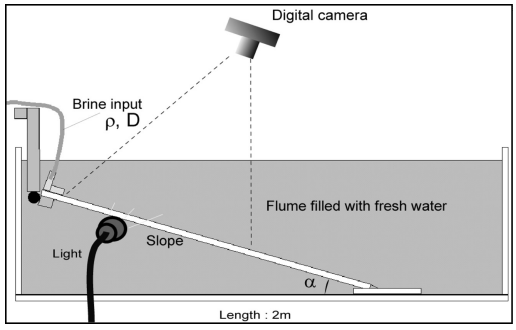

Figure 2. Experimental setup, not to scale.

before reaching the bottom. For small scale experiments, X is less than a few centimetres, even when attempting to lower V_s with very small and light particles. When particles are mixed with the water at the input of our experimental setup, they settle down just a few centimetres after the entrance, and no channel can be formed.

The employ of brine to produce the density contrast figures out this scale problem. Because the brine is transparent, the second benefit of this method is to enable visualization of the bed during the whole experiment, and then to allow us to study the incision dynamics.

3 INCISION DYNAMICS

We have shown in a previous work (Métivier et al. 2005) that a steady-state density current can induce self-channelization. Indeed, in these experiments, the sediment blanket is initially flat. When the brine is introduced, there is a development phase in which the density current spreads over the bed and then the channel inception phase begins. In the meantime, the sediment eroded during the channel formation is deposited at the base of the ramp, and constructs a depositional lobe. Here we present a few aspects of this channel incision dynamics.

3.1 *Measurement method*

In order to perform dynamical acquisitions of the topography, we use an overhead projector to project parallel sinusoidal fringes on the incline. A digital camera takes a picture from above every minute. On these pictures, the height variations induce phase modulations of the sinusoidal signal. At a point A, the phase difference $\Delta\varphi$ due to a sediment layer height h is given by (see figure 3 for notations):

$$\Delta\varphi = \varphi_A - \varphi_B = 2\pi \frac{h}{\lambda . \cos\alpha}$$

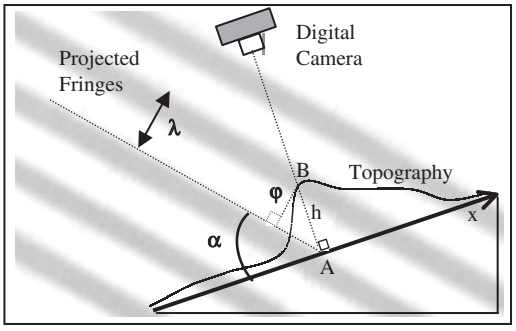

Figure 3. Principle of the optical acquisition technique.

Then with an algorithm based on the Fourier transform we compute a phase demodulation and deduce the contours and their evolution during the experiment. Furthermore, with differences between successive maps, we can elaborate time-varying maps of sedimentation and erosion rates in the system.

3.2 *Results*

Figure 4 shows a typical channel and the time evolution of the sediment layer height for three cross sections. Here is the description of the successive phases observed during such experiments:

The channel inception phase begins rather suddenly, about 15 minutes after the experiment has been started (Fig. 4b, c). Before this moment, the density current was spreading on the bed. Erosion and particle transport were present, but remained weak and relatively well distributed on a large array. Nevertheless we observed that during this development phase the erosion is greater in the middle of the density current than on its sides. Slowly then, the active erosion array is reduced and the density current becomes more focused. This process leads to the beginning of the incision phase.

The first significant incision is located at the top of the ramp. It is followed by a positive feedback mechanism facilitating further erosion. The cross section on figure 4b shows a linear widening phase of 40 minutes. The cross section on figure 4d is taken downstream in comparison with the 4b, and the incision phase is much more abrupt. While, for the 4b cross section, the lateral erosion is responsible for the widening of the sides, on the other hand there is no widening phase for the 4d cross section: the channel is already incised upstream, and this abrupt incision phase is the result of its progradation. This progradation is manifest on the down-slope cross section displayed on figure 4c. An erosion-deposition wave is propagating downstream: both the frontal lobe and the channel incision seem to move forward at the same velocity, which is about 2.5 mm/minute.

In the last phase, the channel width reaches a steady state: the erosion takes place on the bed instead of on the sides. It's a deepening phase. This steady state has been observed with most of the experiments we have made, but not with all of them. It is likely that those experiments were not run for a sufficiently long time.

3.3 *Aspect ratio*

We compared the aspect ratio (i.e. the width over depth ratio) of our experimental channels to natural ones, using the figure of Clark & Pickering (1996), and we found a good agreement (fig. 5). Our values are between 5 and 10, which means that our small-scale channels have morphology similar to natural ones.

3.4 *Meandering*

In some cases, the channel first shows a straight morphology, and then its sinuosity increases through time. We are not currently able to extract the parameter which determines the meandering, but we suspect the initial topography imperfections to play a consequent role in the triggering of this instability.

4 INCISION CONDITIONS

Varying two main parameters, the incline slope and the input flow rate, we ran about twenty experiments in order to see whether or not a channel could be incised. This roughly delineates a sort of phase diagram, plotted on figure 6.

In order to obtain channels, we have to provide high slope and low input flow rate. These two conditions allow the density current to focus instead of spread over the bed. The high slope force the current to flow downward, and the low input flow rate minimizes the jet effects. Both together provide the best conditions for channel incision.

Thus, this diagram is meaningful. However, the slope is not physically relevant here, because this parameter strongly depends on our experimental setup. We wanted to plot this phase diagram with non-dimensional parameters instead, and introduce somehow the erosion power. This could be done taking the shear stress exerted on the bed into account to calculate the Shields parameter.

In order to do this, we have started to study the velocity structure of the current, prior to incision.

5 VELOCITY PROFILE

To better characterize the brine flow and the shear stress on the bed just before the incision phase, we used the same experimental setup as before, without sediment layer on the incline. This way we can have a better

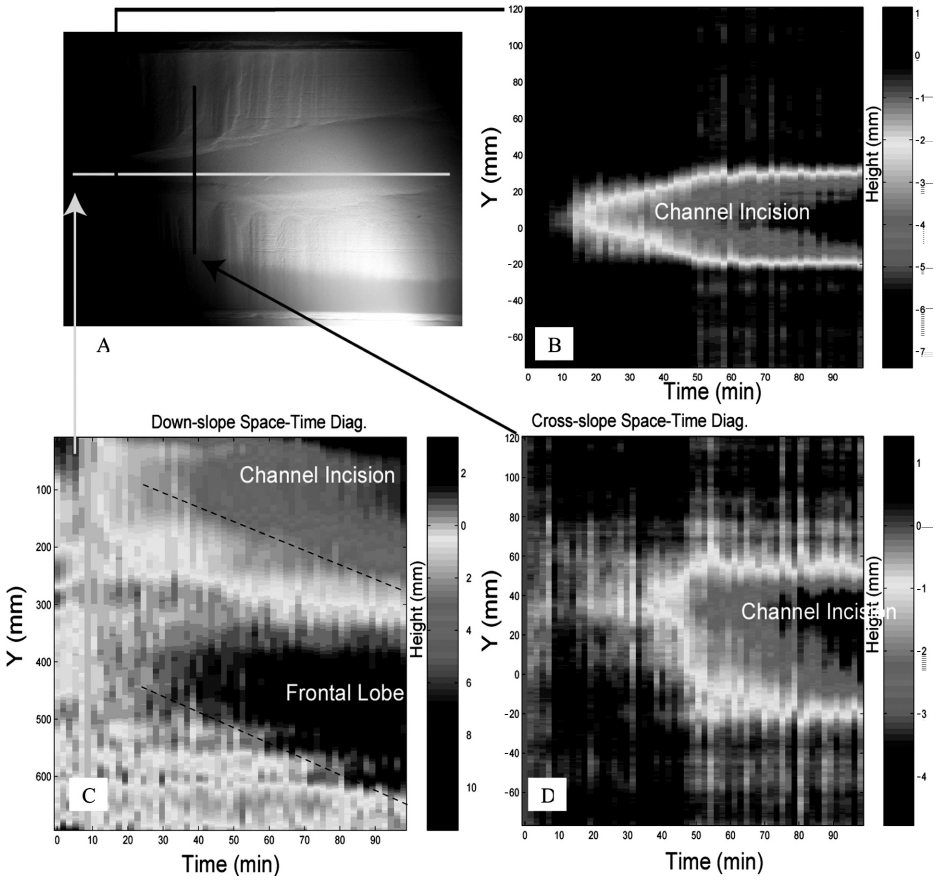

Figure 4. Space-time diagrams of the topography of a typical channel. The left-upper picture shows the channel obtained 100 minutes after the experiment start up, viewed from above (brine entrance is on the left side). Three cross sections are located on this picture. One is down-slope and two are cross-slope. The three other graphs are the space-time diagrams showing the evolution of these cross sections through time. Frontal lobe and channel incision phase are located on the three diagrams. (Parameters: slope = 17°, flow rate = 1.7 g/s, brine density = 1.025).

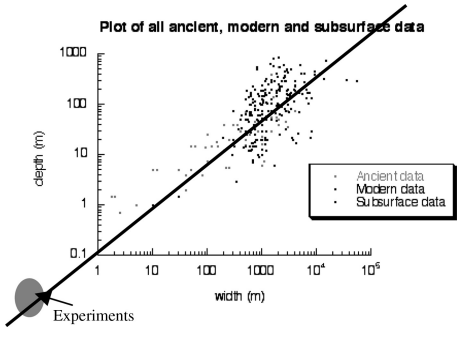

Figure 5. Subaqueous channel aspect ratio, after Clark & Pickering (1996). The dots represent real submarine channels, while the gray area represents the range of our experiments. The line indicates an aspect ratio (width/depth) of 10.

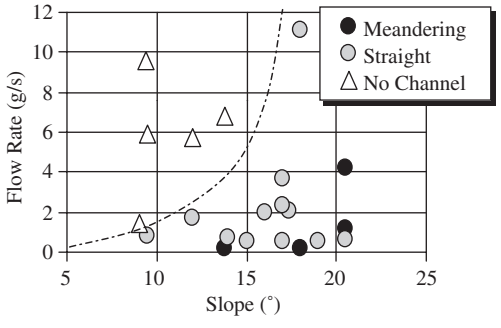

Figure 6. Phase diagram of the channel formation. The solid line has been added as a guide to visualization.

control on the topography, which remains flat to simulate the initial conditions of the with-sediment-blanket experiments.

5.1 *Measurement method*

Here we present the particle-with-shadow tracking technique, a new simple experimental method for measuring the velocity vertical profile, applied on the gravity current with a good accuracy.

We drop some particles in the water over the part of the incline we want to study. The particles sink very slowly because of both their low specific gravity and their small size. Before reaching the bottom, they pass through the brine current and thereby give information on the horizontal velocity field.

The incline is lit by a precise light source, with a small incidence angle. Making close movies of a small part of the incline from above, we track a falling particle and its shadow, on each picture (fig. 7a). The particle height above the plane is deduced directly from the particle-shadow distance. Knowing the particle position in 3D through time, and because the particle traverses the brine flow, we can reconstruct the velocity vertical profile. Only one particle is sufficient to obtain the profile, but the use of several particles for the treatment provides a better accuracy.

The choice for the incidence angle of the light source is consequential: with a very small angle, the shadow is far from the particle, and then a very good accuracy can be achieved when measuring the particle height above the incline. However it becomes more difficult to track the shadow when the particle is high.

The particle-with-shadow tracking is much easier and accurate with the use of space-time diagrams (fig. 7b). These diagrams allow visualizing the evolution of a pixel line with time. Then it is convenient to select and follow falling particles from picture to picture.

5.2 *Results*

Figure 8a shows the vertical profile measured with the tracking method. We managed to obtain it for the lowest part of the density current, where the velocity decreases: all data on this graph are under 0.5 mm high from the bed.

6 SHEAR STRESS MEASUREMENT

We use the downstream velocity profile in order to determine the Shields stresses exerted on the bed during the initial incision phase. We obtain the decreasing

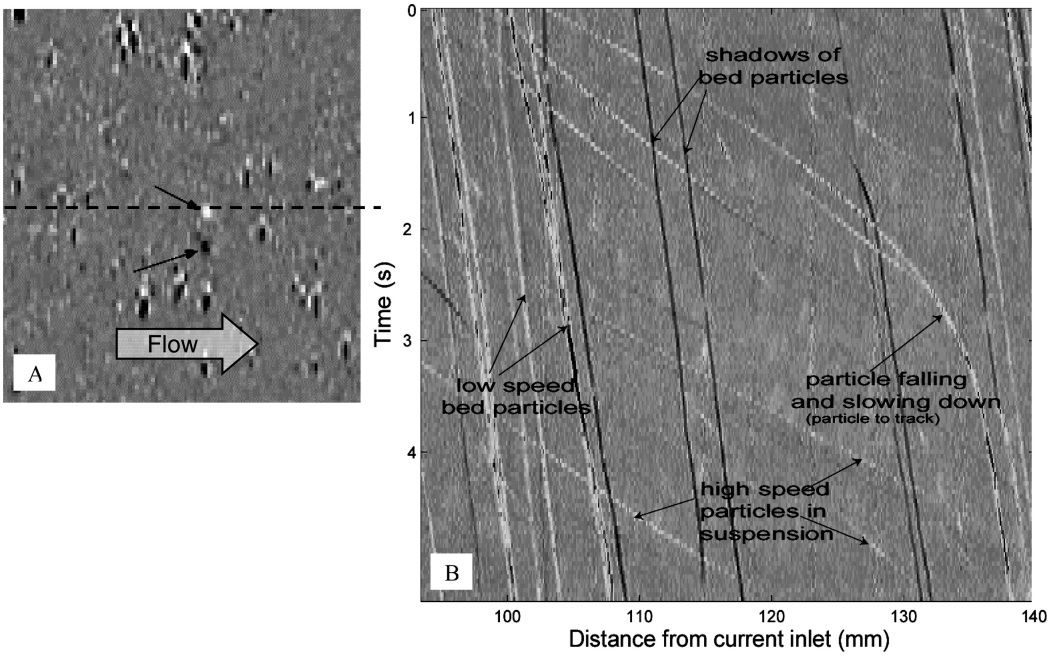

Figure 7. a) Picture extracted from a close movie of the incline taken from above. The arrows point a falling particle with its shadow. The dashed line locates the pixel line used for the space-time diagram. b) Space-time diagram of a down-slope pixel line, showing particles in white and shadows in black.

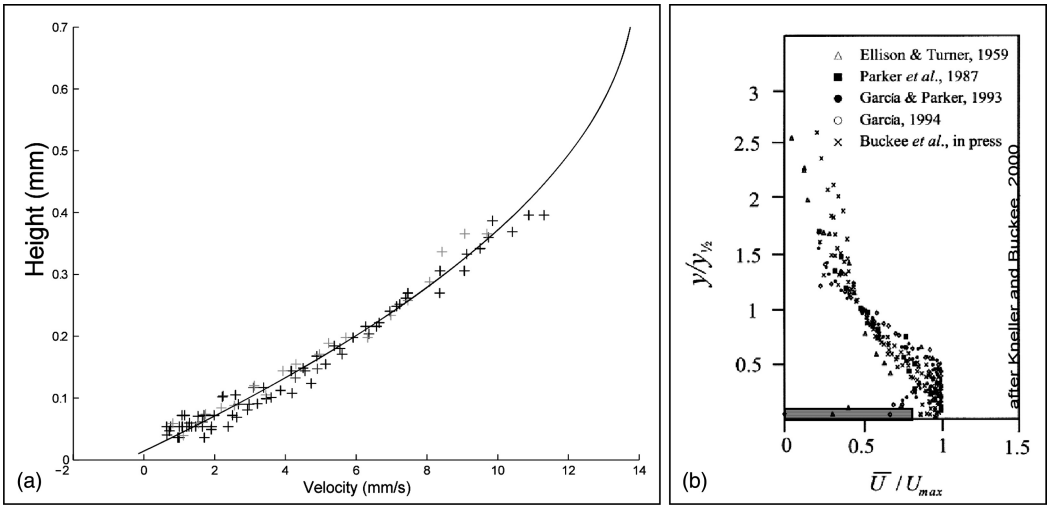

Figure 8. Velocity vertical profiles for gravity currents. a) Lowest part of the profile, obtained using the particle-with-shadow tracking technique on five different particles. Solid line is a 2nd order polynomial fit. (Parameters: slope = 13.7°, flow rate = 0.6 g/s, brine density = 1.025). b) Normalized profiles, after Kneller & Buckee (2000). The gray box locates the area of the profile.

velocity in the lowest part of the flow with a good accuracy. In this part, the Reynolds number is about 1. Thus, the velocity gradient we have located in the viscous sublayer. Then we have direct access to the shear stress τ, using the definition:

$$\tau = \mu \left. \frac{\partial U}{\partial z} \right|_{z=0}$$

Where U is the velocity, z is the height, and μ is the dynamic viscosity.

Figure 9 represents the range of values obtained in our experiments on a Shields diagram. This diagram uses non-dimensional parameters τ^* and D^*:

$$\tau^* = \frac{\tau}{\Delta\rho . g . D . \cos\alpha}$$

$$D^* = D \sqrt[3]{\frac{\Delta\rho . g}{\rho . \nu^2}}$$

Where D is the particle diameter, α is the incline slope, g is the gravity, ν is the cinematic viscosity, ρ is the brine density and $\Delta\rho$ is the particle-brine density contrast. τ^* is the non-dimensional shear stress, and D^* is the non-dimensional particle diameter.

On the same diagram we plotted the Shields curve, which gives, for a given particle diameter, the critical shear stress to provide in order to erode, and we plotted an estimation made after the data of Khripounoff et al. 2003, who reported measurements on natural channels.

In both experimental and natural cases, the shear stresses observed are well above the critical shear stress.

7 FORESIGHTS

We showed that a steady-state density current can produce self-channelization, for a sufficiently high slope and a low input flow rate. After a slow development phase, the incision and widening phase suddenly begins, while a frontal lobe progrades. In some cases, a steady state can finally be obtained.

Our channels have aspect ratios similar to natural ones, and from velocity profiles we measured shear stress values about ten times above the critical shear stress.

Further experiments need to be made in order to better characterize the dense current prior to incision, measuring height, width, velocities and shear stress variations when changing the slope and the flow rate. The velocity profiles obtained have to be extended higher to measure the maximum velocity and the typical height of the current. The effect of dilution by fresh water entrainment at the current inlet has to be investigated in more details to provide better control on the density.

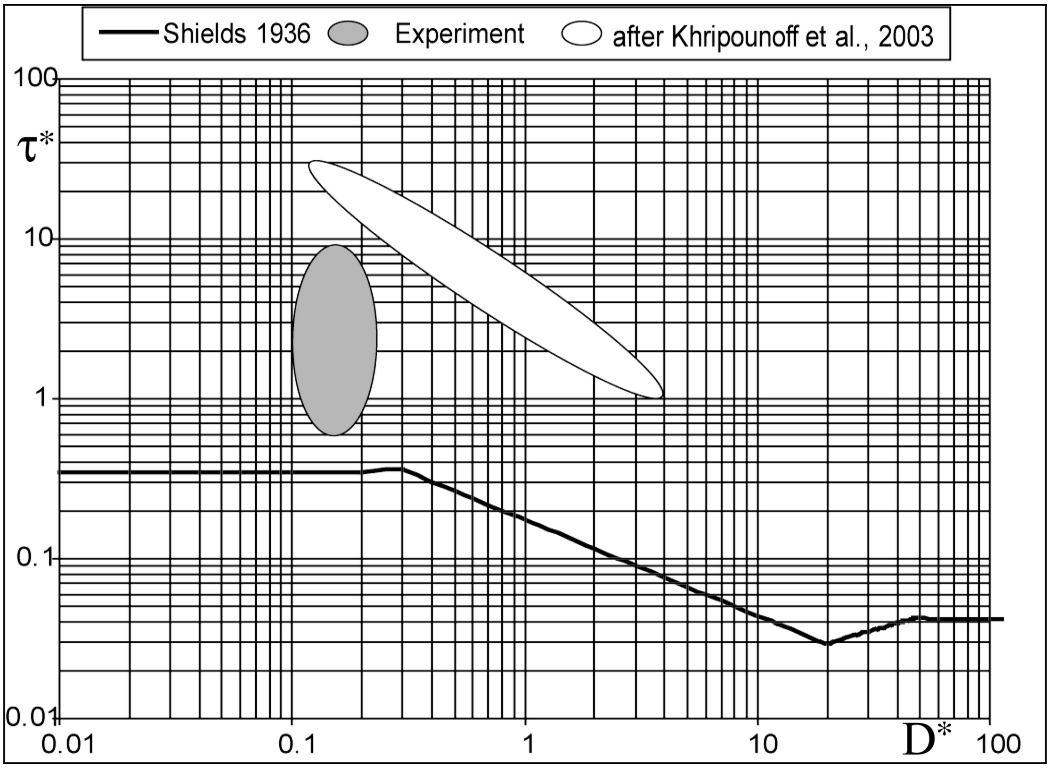

Figure 9. Shields diagram for our experiments and for the Zaïre submarine channel (estimated values after Khripounoff et al. (2003)).

At last, we would like to establish a phase diagram specifying the incision conditions in terms of non-dimensional shear stresses.

REFERENCES

Bonnecaze, R.T. & Lister, J.R. 1999, Particle-driven gravity currents down planar slopes. *Journal of Fluid Mechanics*. 19: 445–467.

Clark, J.D. & Pickering, K.T. 1996, *Submarine Channels: Processes and Architecture*. London: Vallis Press.

Ellison, T.H. & Turner, J.S. 1959, Turbulent entrainment in stratified flows. *Journal of Fluid Mechanics.* 6: 423–448.

Garcia, M.H. & Parker, G. 1993, Experiments on the entrainment of sediment into suspension by a dense bottom current. *Journal of Geophysical Research.* 98: 4793–4807.

Garcia, M.H. 1994, Depositional turbidity currents laden with poorly sorted sediment. *Journal of Hydraulic Engineering.* 120: 1240–1263.

Khripounoff, A. et al. 2003, Direct observation of intense turbidity current activity in the Zaire submarine valley at 4000 m depth. *Marine Geology*. 194: 151–158.

Kneller, B. et al. 1999, Velocity structure, turbulence and fluid stresses in experimental gravity currents. *Journal of Geophysical Research.* 104(C3): 5381–5391.

Kneller, B. & Buckee, C. 2000, The structure and fluid mechanics of turbidity currents: a review of some recent studies and their geological implications. *Sedimentology.* 47(1s): 62–94.

Métivier, F. et al. 2005, Submarine canyons in the bathtub. *Journal of Sedimentary Research.* 75(1): 6–11.

Parker, G. et al. 1987, Experiments on turbidity currents over an erodible bed. *Journal of Hydraulic Research.* 25: 123–147.